Diffusion in liquid aluminium probed by quasielastic neutron scattering

F. Demmel,[1,*] D. Szubrin,[2] W.-C. Pilgrim,[2] and C. Morkel[3]
[1]*ISIS Facility, Rutherford Appleton Laboratory, Didcot, Oxon OX11 0QX, United Kingdom*
[2]*Fachbereich Chemie, Philipps-Universität Marburg, 35032 Marburg, Germany*
[3]*Physikdepartment E21, TU München, 85748 Garching, Germany*
(Received 31 March 2011; published 28 July 2011)

The diffusion coefficient of liquid aluminium has been obtained through coherent quasielastic neutron scattering. The resulting values agree well with calculations derived from the viscosity applying the Stokes-Einstein relation and with *ab initio* calculations. The temperature dependence of the diffusion constant displays an Arrhenius-type behavior with a single activation energy of 274 meV, consistent with results obtained by utilizing embedded atom method potentials.

DOI: 10.1103/PhysRevB.84.014307 PACS number(s): 66.10.−x, 78.70.Nx

I. INTRODUCTION

Aluminium is used in many facets in our daily life and is produced in huge amounts yearly. The production process involves at some stage the processing of the metal in the liquid state and subsequent solidification. Diffusion is an important process during this step which can influence texture and strength. The knowledge and understanding of the diffusion process on a quantitative basis is hence a necessity for successful phase field modeling and could have important consequences on the production process. Surprisingly there is a lack of measurements of the diffusion coefficient for liquid aluminium. The classical capillary method requires suitable radioactive isotopes, which are not available for aluminium. The reported diffusion constants are all based on computational efforts. At first, classical molecular dynamics (MD) simulations using pseudopotentials[1] have been applied. Later on first-principles molecular dynamics[2] and orbital-free *ab initio* MD studies[3] have been performed on the structure and dynamics of liquid aluminium. The scatter of calculated diffusion coefficients asks for input from experiment. One approach to derive diffusion constants is neutron scattering. However, the purely coherent scattering of aluminium provides a more complicate situation.

In the hydrodynamic limit, the simplest ansatz is the well-known solution of Fick's diffusion law which describes the motion of a Brownian particle in space and time and which defines the self-diffusion constant D of a tagged particle. A simple Lorentzian line shape is expected where the half width at half maximum (HWHM) $\Gamma_{1/2}$ is related to the diffusion coefficient by $\Gamma_{1/2} = DQ^2$. Hence, measuring the incoherent scattering function $S_{\mathrm{inc}}(Q,\omega)$ allows for the determination of the self-diffusion coefficient of the liquid. This approach for determining diffusion constants has often been applied for liquid metals and alloys.[4–6]

The situation is more intricate if the sample nuclei scatter only or mostly coherent. Coherent neutron scattering provides insight into the collective movements of the particles. In the hydrodynamic limit, the scattering function is given by a combination of three Lorentzians, neglecting a small asymmetry term.[7] Two Brillouin lines originate from density fluctuations and the quasielastic Rayleigh line stems from temperature fluctuations. The Brillouin lines disperse with the velocity of sound and can be followed far into the microscopic region.[8] For larger momentum transfers or when length scales of atomic diameters are probed, the quasielastic line shows a narrowing around the structure factor maximum, known as deGennes narrowing.[9] In the time domain, the intermediate scattering function for density fluctuations $F(Q,t)$ demonstrates a slowing down at the structure factor maximum. DeGennes derived the frequency moments for the scattering function and found that the second moment is given by: $\Omega_0^2 = \frac{k_B T Q^2}{mS(Q)}$. The moments are a measure of the spread of the spectra and show according to the calculation a decrease of the width when the structure factor $S(Q)$ reaches its maximum. In a simple picture, it costs time for a density fluctuation to relax on a next-neighbor length scale due to a necessary rearrangement of the surrounding particles. This structural slowing down is manifested in the relaxation time through the structure factor $S(Q)$.

Within kinetic theory, the line width at the structure factor maximum has been related to a diffusion process, which enables the density fluctuations to decay.[10] Within this formulation, the following connection between the Enskog self-diffusion coefficient D_E of a hard sphere fluid and the measured half width at half maximum $\Gamma_{1/2}$ has been established:[10]

$$\Gamma_{1/2} = \frac{D_E Q^2 d(Q\sigma)}{S(Q)}, \tag{1}$$

where $d(Q\sigma) = \mathbf{(}1 - j_0(Q\sigma) + 2j_2(Q\sigma)\mathbf{)}^{-1}$ is given by a combination of spherical Bessel functions j_l of order l and σ denotes the hard sphere diameter. This relation strongly resembles the hydrodynamic description of the self-diffusion process, where the structure factor $S(Q)$ takes into account the slowing down of a diffusion process at next-neighbor distances. On these length scales of one atom diameter, the relaxation of density fluctuations resembles single particle behavior.[11] It has been shown, e.g., that the calculated line widths around the structure factor maximum of noble gases agree with measured values over a wide range of densities. The same relation has also been applied to liquid alkali metals. It was shown that for liquid cesium[12] and liquid rubidium,[13] the derived diffusion coefficients are consistent with the calculated Enskog value near the melting point and for liquid rubidium even up to the boiling point.[14]

However, the Enskog model calculates the diffusion coefficient D_E of a hard sphere system by taking into account

only binary collisions. The neglect of more complex correlated collisions is the reason for deviations of the macroscopic self-diffusion constant at high and low densities. At high densities, coupling to density fluctuations with wave numbers near the structure factor maximum hinders the diffusion process and hence reduces the diffusion constant.[15] In contrast, at low densities, it is the coupling to vortex backflow which enhances the diffusion constants. Through a comparison between simulated self-diffusion coefficients and calculated Enskog values over a large range of densities, a correction curve was reported:[16]

$$D = D_E\left(1+0.05403\left(\frac{V_o}{V}\right)+6.3656\left(\frac{V_o}{V}\right)^2-10.9425\left(\frac{V_o}{V}\right)^3\right). \quad (2)$$

The correction is given as a function of relative density $V_0/V = n\sigma^3/\sqrt{2}$, where V_0 denotes the closed packed volume. For example, these corrections describe quantitatively the diffusion behavior of liquid sodium over a wide range of densities very well.[5] A kinetic theory with inclusion of correlated collisions has been given first by Cukier and Mehaffey[17] for a hard sphere liquid and later by Wahnstrom and Sjogren[18] for continuous potentials. The characteristic feature of Eq. (2) is well displayed, namely, the reduction of D/D_E near the melting point via the cage effect and an enhancement of D/D_E due to transverse currents at higher temperatures with a typical maximum near $V_0/V = 0.4$.[19] With all these corrections, which seem to work to a high accuracy for some systems, one has to keep in mind that the self-diffusion constant is extracted from a coherent quantity. Only comparison with sophisticated *ab initio* simulations or new experimental data will tell to which extent these corrections are correct for liquid aluminium.

II. EXPERIMENTAL DETAILS

Aluminium is a pure coherent scatterer with an incoherent cross section of less than 0.01 barn compared to the coherent cross section of 1.495 barn. Because aluminium alloys with almost all metals alumina were chosen as sample can material. The same cell material was used in an early structure factor measurement.[20] A cylindrical cell with an outer diameter of 25 mm and an inner diameter of 20 mm was filled with a 99.999% pure aluminium rod. The alumina cell was closed with a niobium cap glued onto the alumina cell by a ceramic high temperature glue, which is stable up to 1800 K. The sample was installed in a furnace and heated with a stability of ±2 K. The melting point of aluminium is 933.5 K. Measurements have been performed between the melting point and 1193 K in about 50 K steps. The sample weight did not change during the experiment.

The spectra of liquid aluminium have been measured at the IRIS-spectrometer of the ISIS Facility, UK. A spectrometer configuration with an end energy of 7.38 meV was chosen, which provided an energy resolution of 0.055 meV (FWHM). This good energy resolution well separated from the liquid aluminium dynamics facilitates the correction of the empty can contribution. The Q-resolution was about ±0.04 Å^{-1}. The structure factor maximum of liquid aluminium occurs at

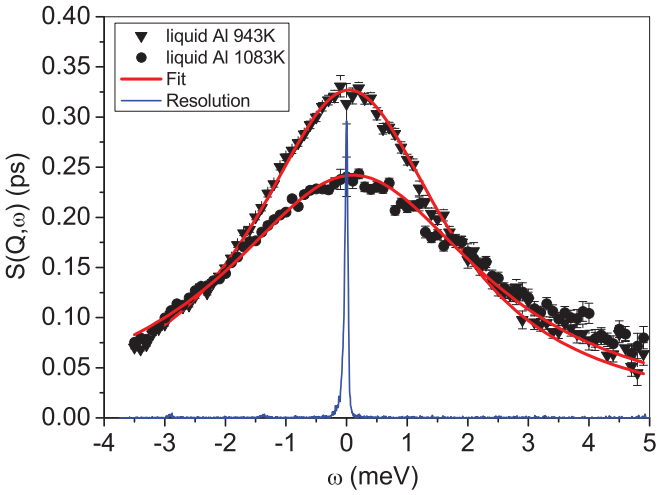

FIG. 1. (Color online) Two spectra of liquid aluminium are depicted for a Q-value at the peak of the structure factor. The line shows the fit with a Lorentzian. Included is the resolution from the spectrometer, which is about a factor 40 smaller than the width of the spectra.

$Q_0 = 2.7$ Å^{-1}. Strong scattering powder lines of alumina which could affect the data analysis are outside this Q-range.

In Fig. 1, two spectra at $Q_0 = 2.7$ Å^{-1} are displayed including the measured resolution function. The overall line shape, shown as a line, is reproduced by one Lorentzian. The contribution of the spectrometer resolution is so small that a convolution with the resolution function was not performed for the fit. With increasing temperature, the spectra broaden and fill the available dynamic range of the spectrometer which was from −3.5 to +5 meV. The data analysis included monitor normalization, empty cell subtraction, absolute calibration with a vanadium standard, and conversion into constant Q-spectra. Absorption coefficients for the empty cell subtraction have been calculated according to a method of Paalman and Pings.[21] The multiple scattering contribution is small at the structure factor maximum and was not corrected. To describe the line shape and to extract the line widths, a fit with a single Lorentzian function was used.

III. RESULTS AND DISCUSSION

Fitting Lorentzians to constant Q spectra around the structure factor maximum delivers the half width at half maximum $\Gamma_{1/2}(Q)$. Figure 2 displays the result for $T = 943$ K. Included in the figure is the structure factor of liquid aluminium obtained by x-ray diffraction.[22] It demonstrates well the correspondence between the structure and the slowing down of the dynamics. To extract the diffusion coefficient D_E, Eq. (1) was fitted to the widths around the structure factor maximum in a Q-range between 2.4 and 2.9 Å^{-1}. As input parameters, the temperature-dependent $S(Q)$ values and the hard sphere parameter σ are needed. For $S(Q)$, the x-ray literature data from Waseda have been used which cover three temperatures: 943, 1023, and 1323 K.[22] The values for the missing temperatures have been interpolated. It has to be noted

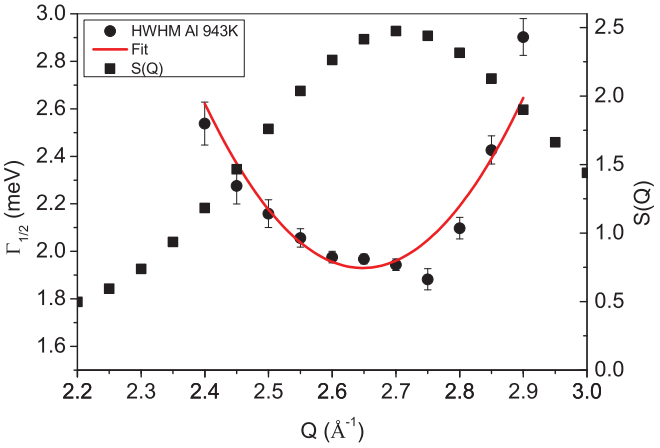

FIG. 2. (Color online) The HWHMs of liquid aluminium at 943 K are displayed together with literature values of the structure factor $S(Q)$ (Ref. 22). The line is a fit through the widths according to Eq. (1).

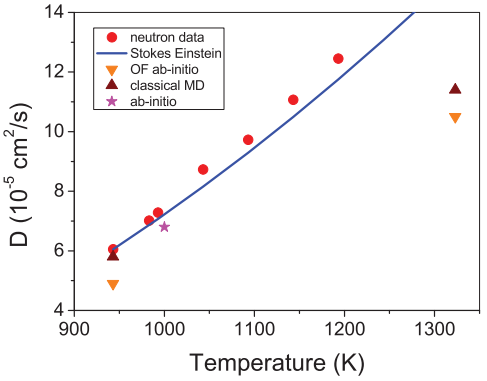

FIG. 3. (Color online) The derived diffusion coefficients D are shown with rising temperature. The line denotes the calculated diffusion values using the Stokes-Einstein relation. The star denotes a value from an *ab initio* calculation (Ref. 2), the down triangles are from an orbital-free (OF) *ab initio* calculation and the up triangles from a classical MD (Ref. 3).

that the $S(Q)$ peak values from the neutron diffraction work[20] are lower than the corresponding x-ray data, whereas the newer neutron diffraction data[23] seem to differ less. The hard sphere parameter σ has been derived from a Percus-Yevick fit[7] to $S(Q)$ around the main structure peak. The obtained value for $\sigma = 2.53$ Å at $T = 943$ K is consistent with used values in simulations.[2,24] A theoretical study on the potential of liquid aluminium concluded that a hard sphere diameter of $\sigma = 2.57$ Å approximates well the structure factor.[25] The fit delivers a slight reduction of the hard sphere parameter with rising temperature which reflects the softness of the repulsive part of the potential. The resulting temperature-dependent parameters are given in Table I. Then Eq. (2) was applied to the Enskog values D_E to obtain the diffusion constants D. The table includes also the Enskog diffusion values derived from the neutron data according to Eq. (1) and the corrected diffusion constants D.

In Fig. 3, the obtained diffusion coefficients D are depicted (circles) and compared with results from simulations and derived values from the viscosity. An indirect method to obtain a diffusion constant is based on the Stokes-Einstein relation:[26] $D = \frac{k_B T}{2\pi \eta d_{\text{eff}}}$. Here k_B denotes the Boltzmann constant, T is the temperature, d_{eff} is an effective atomic diameter, and η is the viscosity. The temperature-dependent viscosity was taken from a recent compilation of data for liquid aluminium[27]

TABLE I. The table provides the values for the structure factor peak $S(Q_0)$, the hard sphere parameter $\sigma(T)$, and the diffusion coefficients D_E and D.

T (K)	$S(Q_0)$	σ (Å)	D_E (10^{-5} cm^2/s)	D (10^{-5} cm^2/s)
943	2.5	2.53	6.5 ± 0.02	6.06
993	2.4	2.518	7.4 ± 0.02	7.29
1043	2.32	2.507	8.5 ± 0.02	8.73
1093	2.26	2.5	9.2 ± 0.02	9.73
1143	2.2	2.494	10.2 ± 0.05	11.07
1193	2.15	2.487	11.2 ± 0.07	12.45

and for d_{eff}, the hard sphere parameters from Table I were applied. The so derived diffusion constant, which is based on macroscopic data, is included as a line and agrees well with D from neutron scattering at next-neighbor distances.

These values are compared with results from *ab initio* and classical MD simulations. A first-principles calculation from Alfe and Gillan reports a diffusion constant of $D = 6.8 \times 10^{-5}$ cm^2/s[2] at the experimental density (star), which agrees well with our values. Gonzales *et al.* used an orbital-free *ab initio* method to calculate the dynamics in liquid aluminium for two temperatures.[3] For comparison, a local pseudopotential was used in a classical MD simulation. At the melting point, the diffusion coefficient derived by the pseudopotential lies near to the experimental values, whereas D from using the orbital-free *ab initio* MD is about 20% lower. Surprisingly, both methods deliver values at the high temperature which seem to be too low compared with the expectations from the experimental data and from the Stokes-Einstein calculation. Later on the same group performed a Kohn-Sham *ab initio* calculation on liquid aluminium and reported the same diffusion coefficient $D = 6.8 \times 10^{-5}$ cm^2/s (Ref. 28) as in Ref. 2. Simulation potentials derived by the embedded atom method (EAM) deliver diffusion coefficients between $D = 3.14 \times 10^{-5}$ and $D = 5.5 \times 10^{-5}$ cm^2/s near the melting temperature, strongly dependent on the exact implementation of the potential.[29]

In Fig. 4, the temperature-dependent diffusion coefficient $D(T)$ is presented in a logarithmic scale. Assuming an Arrhenius-type behavior $D = D_0 \exp(-\frac{E}{k_B T})$ for the diffusion process, an activation energy E can be derived. The fit describes the data points well, so one activation energy is sufficient to describe the diffusion process in this temperature range. The derived activation energy is $E = 274 \pm 4$ meV and the prefactor is $D_0 = 179 \pm 11 \times 10^{-5}$ cm^2/s. Activation energies have been obtained from classical MD simulations using potentials derived by the embedded atom method (EAM).[29] A range of activation energies between 259 and 310 meV has been reported due to different implementations of the EAM potential. $D(T)$ values calculated with one of the potentials ($E_A = 260$ meV), believed to describe the structure best, have been included into Fig. 4 as a dashed line. The overall

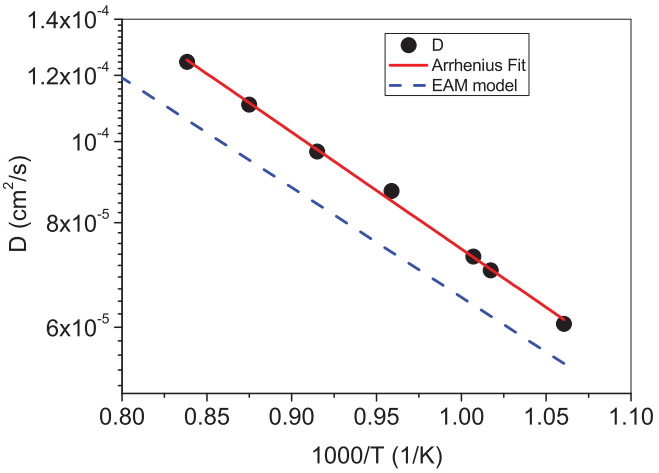

FIG. 4. (Color online) The diffusion coefficient are given in a logarithmic scale. A fit with an Arrhenius-type activation process describes the temperature dependence sufficiently well. The dashed line represent the simulated $D(T)$ values from a particular EAM potential (Ref. 29).

diffusion coefficients are smaller, which might be related to different temperatures between simulation and experiment, but the activation energy agrees well with the simulation.

The diffusion coefficients in the Enskog model and the correction provided by Eq. (2) are all based on the assumption of hard spheres. Aluminium has valence three and pseudopotential theory predicts distinct changes in the potential compared to the simple alkali metals.[30] However, the agreement of the derived diffusion coefficients with values of the calculations indicate that liquid aluminium can still be regarded as a hard sphere-like liquid in respect of its diffusion behavior. This might be related to the fact that in a dense liquid, mainly the strong repulsive part of the potential is probed by the particles, which might be very similar in many metals. For liquid aluminium, it was shown that a hard sphere potential can approximate the true potential quite well, reflected in the structure factor.[25]

IV. CONCLUSIONS

Experimental diffusion coefficients of liquid aluminium have been obtained from coherent quasielastic neutron scattering. The decay of the density fluctuations near the structure factor maximum is a process which is strongly related to a self-diffusion step. This resemblance was used to derive diffusion constants for several temperatures. The derived diffusion constant agrees well with an *ab initio* result near the melting point and values calculated with the Stokes-Einstein relation. The temperature dependence suggests a single activation process described by an Arrhenius relation. These first experimental diffusion constants of liquid aluminium might provide an important input data set for simulation work and phase field modeling. The outlined method to derive diffusion coefficient from coherent quasielastic neutron scattering might be applicable to many more metals with a potential which resembles a hard sphere-like potential.

*franz.demmel@stfc.ac.uk

[1] I. Ebbsjo, T. Kinell, and I. Waller, J. Phys. C **13**, 1865 (1980); G. Jacucci, R. Taylor, A. Tenenbaum, and N. van Doan, J. Phys. F: Met. Phys. **11**, 793 (1981).
[2] D. Alfe and M. J. Gillan, Phys. Rev. Lett. **81**, 5161 (1998).
[3] D. J. Gonzalez, L. E. Gonzalez, J. M. Lopez, and M. J. Stott, Phys. Rev. B **65**, 184201 (2002).
[4] Chr. Morkel and W. Gläser, Phys. Rev. A **33**, 3383 (1986).
[5] W.-C. Pilgrim and C. Morkel, J. Phys. Condens. Matter **18**, R585 (2006).
[6] A. Meyer, Phys. Rev. B **81**, 012102 (2010); **66**, 134205 (2002).
[7] J. P. Boon and S. Yip, *Molecular Hydrodynamics* (McGraw-Hill, New York, 1980).
[8] T. Scopigno, U. Balucani, G. Ruocco, and F. Sette, Phys. Rev. E **63**, 011210 (2000).
[9] P. G. deGennes, Physica **25**, 825 (1959).
[10] E. G. D. Cohen, P. Westerhuijs, and I. M. de Schepper, Phys. Rev. Lett. **59**, 2872 (1987).
[11] W. Montfrooij and I. deSchepper, *Excitations in simple liquids, liquid metals and superfluids* (Oxford University Press, Oxford, 2010).
[12] T. Bodensteiner, Chr. Morkel, W. Gläser, and B. Dorner, Phys. Rev. A **45**, 5709 (1992).
[13] F. Demmel, A. Diepold, H. Aschauer, and C. Morkel, Phys. Rev. B **73**, 104207 (2006).
[14] W.-C. Pilgrim, R. Winter, F. Hensel, C. Morkel, and W. Gläser, Ber. Bunsen. Phys. Chem. **95**, 1133 (1991).
[15] U. Balucani and M. Zoppi, *Dynamics of the Liquid State* (Clarendon Press, Oxford, 1994).
[16] J. J. Erpenbeck and W. W. Wood, Phys. Rev. A **43**, 4254 (1991).
[17] R. I. Cukier and J. R. Mehaffey, Phys. Rev. A **18**, 1202 (1978).
[18] G. Wahnstrom and L. Sjogren, J. Phys. C **15**, 401 (1982).
[19] C. Morkel and W.-C. Pilgrim, J. Non-Cryst. **312–314**, 128 (2002).
[20] J. M. Stallard and C. M. Davis, Phys. Rev. A **8**, 368 (1973).
[21] H. H. Paalman and C. J. Pings, J. Appl. Phys. **33**, 2635 (1962).
[22] Y. Waseda, *The Structure of Non-Crystalline Materials* (McGraw-Hill, New York, 1980).
[23] S. Takeda, S. Harada, S. Tamaki, and Y. Waseda, J. Phys. Soc. Jpn. **60**, 2241 (1991).
[24] T. Gaskell, J. Phys. F **16**, 381 (1986).
[25] J. Hafner, Phys. Rev. A **16**, 351 (1977).
[26] J. P. Hansen and I. R. McDonald, *Theory of Simple Liquids* (Academic Press, London, 2006), p. 192.
[27] M. J. Assael, K. Kakosimos, R. M. Banish, J. Brillo, I. Egry, R. Brooks, P. N. Quested, K. C. Mills, A. Nagashima, Y. Sato, and W. A. Wakeham, J. Phys. Chem. Ref. Data **35**, 285 (2006).
[28] M. M. G. Alemany, L. J. Gallego, and D. J. Gonzalez, Phys. Rev. B **70**, 134206 (2004).
[29] C. A. Becker and M. J. Kramer, Modelling Simul. Mater. Sci. Eng. **18**, 074001 (2010).
[30] J. Hafner and V. Heine, J. Phys. F **13**, 2479 (1983).